RESEARCH ARTICLE

Lithium-Ion Batteries

Energy & Environmental Materials WILEY

A Sustainable Direct Recycling Method for LMO/NMC Cathode Mixture from Retired Lithium-Ion Batteries in EV

*Yu Wang, Kang Shen, and Chris Yuan**

Direct recycling methods offer a non-destructive way to regenerate degraded cathode material. The materials to be recycled in the industry typically constitute a mixture of various cathode materials extracted from a wide variety of retired lithium-ion batteries. Bridging the gap, a direct recycling method using a low-temperature sintering process is reported. The degraded cathode mixture of LMO ($LiMn_2O_4$) and NMC ($LiNiCoMnO_2$) extracted from retired LIBs was successfully regenerated by the proposed method with a low sintering temperature of 300°C for 4 h. Advanced characterization tools were utilized to validate the full recovery of the crystal structure in the degraded cathode mixture. After regeneration, LMO/NMC cathode mixture shows an initial capacity of 144.0 mAh g^{-1} and a capacity retention of 95.1% at 0.5 C for 250 cycles. The regenerated cathode mixture also shows a capacity of 83 mAh g^{-1} at 2 C, which is slightly higher compared to the pristine material. As a result of the direct recycling process, the electrochemical performance of degraded cathode mixture is recovered to the same level as the pristine material. Life-cycle assessment results emphasized a 90.4% reduction in energy consumption and a 51% reduction in PM2.5 emissions for lithium-ion battery packs using a direct recycled cathode mixture compared to the pristine material.

1. Introduction

Electric vehicles are all powered by lithium-ion batteries. The cathode materials of lithium-ion batteries have evolved from low-energy density and low-cost LMO with a spinel structure to high-cost, Ni-rich layered materials to meet the increasing demand for the driving range of electric vehicles. Typically, lithium-ion batteries reach their end-of-life after 5–10 years of operation.[1] By the end of 2024, 360 000 tons of lithium-ion batteries will be retired from electronic devices and electric vehicles and this number is expected to rapidly increase to 1.22 million tons by 2030.[2] The cathode, rich in high-value lithium and transition metals such as Ni, Co, and Mn, accounts for over 35% of the total cost of lithium-ion batteries. Thus, the recycling of cathode materials from spent lithium-ion batteries is crucial for cost reduction, sustainability enhancement, and the mitigation of environmental impacts associated with the disposal of spent lithium-ion batteries. Conventional recycling methods for the degraded cathode materials are pyrometallurgy and hydrometallurgy. The pyrometallurgy method crushes and smelts the end-of-life lithium-ion batteries and reclaims the valuable metals in the form of alloy via complicated purification and separation processes.[3] The hydrometallurgical process employs a multi-step acid leaching and sedimentation to transform valuable metals from degraded cathode materials into metal compound deposits.[4] These methods are energy-intensive and involve a large amount of chemical usage, leading to the generation of waste gas and solutions. Furthermore, the products of pyrometallurgy and hydrometallurgy require additional synthesis processes to produce pristine cathode materials for lithium-ion batteries. To address these challenges, direct recycling methods have been proposed to regenerate degraded cathode materials with low energy consumption, chemical usage, and environmental impact. The direct recycling methods can effectively recover the structural degradation, restoring the electrochemical performance of degraded cathode materials to the level of the pristine material. The direct recycling methods for single cathode material have been intensively investigated so far. Wu et al. introduced a cost-effective direct recycling technique, successfully restoring lithium loss in degraded LMO through a 30-min magnetic stirring in a lithium-enriched solution.[5] Furthermore, Gao et al. explored the effect of the LiOH concentrations on the regeneration efficiency of degraded LMO in the hydrothermal relithiation method.[6] Meng et al.[7] proposed a direct recycling method that involves mechanochemical activation of degraded NMC111 through ball milling, followed by regeneration via solid-state sintering. Yu et al.[8] developed a low-temperature hydrothermal relithiation process, regenerating degraded NMC111 with green additives and lithium salts at 100°C. The direct recycling methods enable reuse of the regenerated cathode materials in the production of new lithium-ion batteries.

The current direct recycling methods for regenerating single cathode materials do not entirely align with the broader requirements of the battery materials recycling industry. In practical applications, degraded materials are obtained by dismantling and crushing large quantities of retired lithium-ion batteries with different compositions, geometries, dimensions, masses, and electric capacities.[9] As a result, the extracted degraded powder typically contains various types of cathode materials, such as LMO, NMC, etc.[10] The specific types of cathode materials and their weight ratio in the cathode mixture are often unknown. Physical separation of the cathode mixture is challenging and not cost-effective due to the similar composition and morphology of each component. Hence, there is an urgent

Y. Wang, Dr. K. Shen, Dr. C. Yuan
Laboratory of Sustainable Energy Manufacturing, Case Western Reserve University, 10900 Euclid Ave, Cleveland, Ohio 44016, USA
E-mail: chris.yuan@case.edu
The ORCID identification number(s) for the author(s) of this article can be found under https://doi.org/10.1002/eem2.12863.

DOI: 10.1002/eem2.12863

need to develop a direct recycling method capable of regenerating the cathode mixture with different components and weight ratios to reduce costs, mitigate environmental impact, and enhance sustainability. However, due to the different usage conditions and remaining battery life, the cathode materials in the mixture undergo various degradation mechanisms, resulting in different lithium stoichiometry and structural degradation. LMO with a stable spinel structure undergoes lithium loss in most circumstances, while NMC with a layered structure not only experiences lithium loss but also structural degradation after long-term cycling.[11,12] This degradation variation results in the degraded materials having different thermal stability, necessitating an in-depth investigation of the direct recycling method to regenerate all cathode materials in the mixture and avoid decomposition.

In the early stage of electric vehicles, LMO/NCM cathode mixture was widely used in electric vehicles to balance the requirements of energy density, power performance, and the cost. $LiMn_2O_4$ (LMO) is an attractive cathode material, primarily due to its low cost, environmental friendliness, and easy synthesis process.[13] The three-dimensional spinel structure of LMO offers robust channels that facilitate the efficient intercalation and de-intercalation of Li^+ ions, making it well-suited for rapid charging and discharging.[14] $LiNiCoMnO_2$ (NMC), on the other hand, is a layered-structure cathode material known for its high capacity, which enhances energy performance when mixed with LMO.[15] To date, large amounts of lithium-ion batteries using LMO/NCM cathode mixture have reached their end-of-life and needed to be recycled. It is noted that LMO and NMC exhibit different degradation mechanisms due to their distinct crystal structures. The degradation of LMO is mainly attributed to lithium loss resulting from the stability of the spinel structure. In addition to the lithium loss, NMC also undergoes the structural degradation, such as cation mixing and formation of rock-salt layer. Thus, LMO/NMC cathode mixture extracted from retired lithium-ion battery pack in Chevrolet Volt is used in this study to investigate the direct recycling process for degraded cathode mixture.

In this study, a direct recycling method using a one-step sintering process has been developed to regenerate degraded LMO/NMC cathode mixture. This method effectively restores the crystal structure and stoichiometry of the degraded cathode mixture with over 60% capacity loss from EV operations. The regenerated LMO/NMC cathode mixture exhibits a slightly higher electrochemical performance compared to the pristine material, as evidenced by improvements in initial capacity, cycling performance, rate capability, and impedance distribution. The outcomes of this study provide crucial insights into the recycling of spent lithium-ion batteries, showcasing its potential to fulfill the practical demands of the industry.

2. Results

The direct recycling processes of the degraded LMO/NMC cathode mixture extracted from the retired lithium-ion battery packs and the recovery of corresponding material degradation are shown in **Figure 1**. The cathode mixture has undergone significant degradation due to the long-term cycling during the operation of electric vehicles, resulting in over 60% capacity loss. This capacity loss can be attributed to two main degradation mechanisms: lithium loss and structural degradation. In the regeneration process, $LiNO_3$ was utilized as the lithium source to replenish the lithium loss in the degraded cathode mixture. Given the melting point of $LiNO_3$ at 255°C, the regeneration temperature was set at 300°C. At this temperature, lithium became mobile within the molten $LiNO_3$, allowing Li^+ ions to be re-inserted into the crystal structure of the degraded cathode mixture. Meanwhile, structural degradations, including cation mixing of Li^+/Ni^{2+} and the formation of rock-salt layers on the particle surface that hinder Li^+ migration, were recovered by the thermal treatment. The regeneration reactions that occur in the direct recycling process are shown in Equation 1 and 2.

$$Li_{1-x}Mn_2O_4 + xLiNO_3 \rightarrow LiMn_2O_4 + xNO_2 + \frac{x}{2}O_2 \quad (1)$$

$$Li_{1-x}Ni_{0.33}Co_{0.33}Mn_{0.33}O_2 + xLiNO_3 \rightarrow LiNi_{0.33}Co_{0.33}Mn_{0.33}O_2 + xNO_2 + \frac{x}{2}O_2 \quad (2)$$

To identify the initial composition of the cathode mixture and its corresponding weight ratio, energy-dispersive X-ray spectroscopy (EDS) analysis was utilized to determine the atomic ratios of nickel (Ni), cobalt (Co), and manganese (Mn) in the degraded cathode

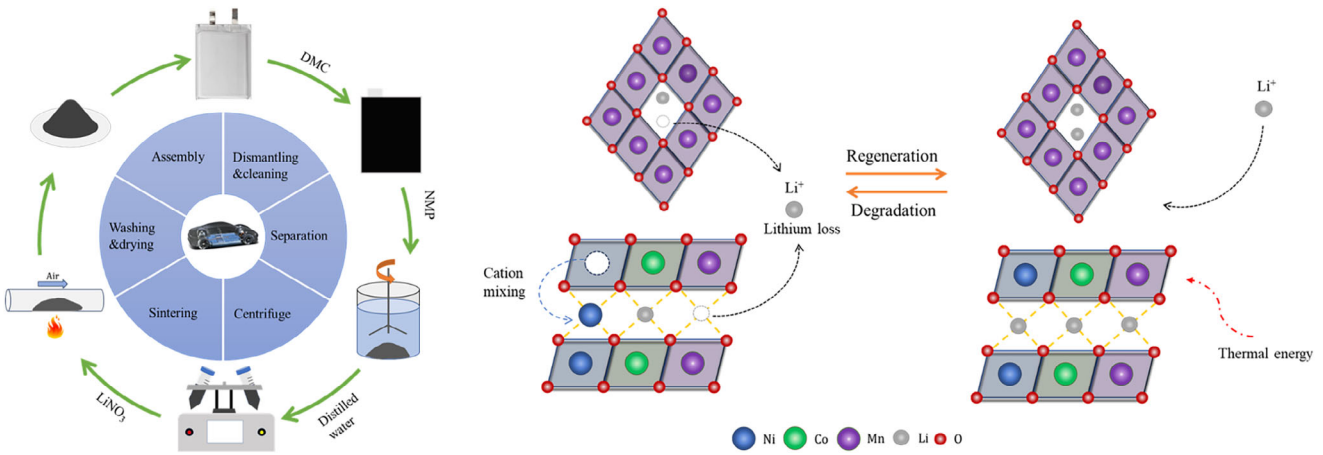

Figure 1. The direct regeneration processes of degraded LMO/NMC cathode mixture.

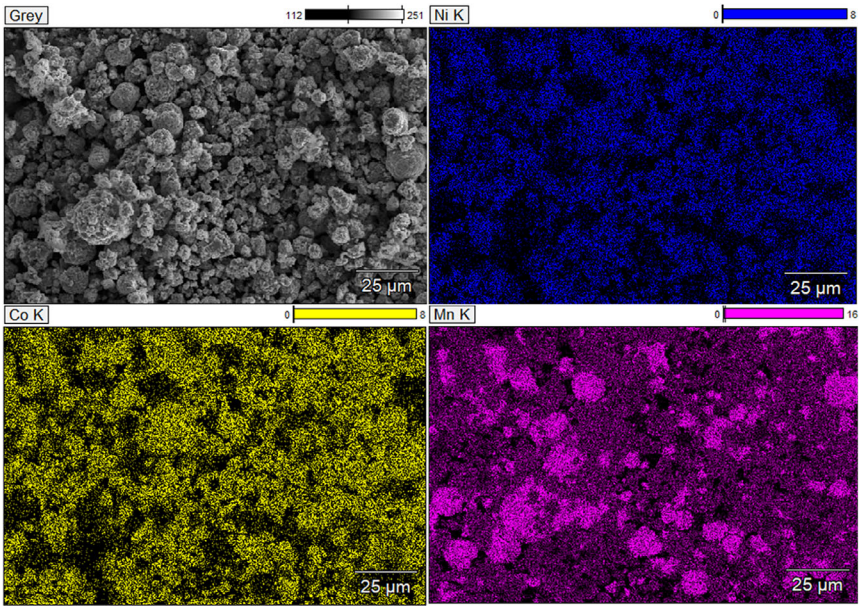

Figure 2. SEM image of degraded LMO/NMC cathode mixture and EDS mappings.

mixture retrieved from the retired EV battery. The scanning electron microscope (SEM) image of the degraded LMO/NMC cathode mixture, along with the corresponding elemental mappings of Ni, Co, and Mn, is presented in **Figure 2**. The elemental mapping revealed a uniform distribution of Ni, Co, and Mn across areas with similar brightness in the Ni, Co, and Mn mappings, consistent with the stoichiometric molar ratio in NMC111. In contrast, regions highlighted in the Mn mapping but absent in the Ni and Co mappings indicate areas containing only Mn, showing the presence of LMO. In the cathode mixture, Mn exhibited the highest atomic ratio at 24.11%, while Ni and Co displayed similar ratios of 10.03% and 9.79%, respectively. Based on elemental ratios, the weight ratio of LMO to NMC in the cathode mixture is 3:7. Carbon (C) and silicon (Si), identified in the mixture, are attributed to XRD substrate, and can be disregarded in the analysis. The post-treatment purification process of the cathode mixture effectively eliminated aluminum (Al), which originated from the aluminum foil debris during the separation process.

SEM was carried out to investigate the particle morphology of the degraded LMO/NMC cathode mixture before and after the regeneration process. SEM images of the degraded and regenerated mixture are shown in **Figure 3**a,b, respectively. Based on the results of elemental mapping in EDS, particles with an average diameter of 20 µm are classified as NMC, while those with an average diameter of 10 µm are identified as LMO. In the degraded cathode mixture, LMO particles maintain their original spherical structure, in contrast to most NMC particles which exhibit fragmentation into smaller particles. The difference in particle morphologies of LMO and NMC is attributed to their distinct crystal structures. The spinel structure of LMO enables it to withstand large stress during lithium insertion and de-insertion, resulting in stress predominantly propagating along the boundary of single particles. This leads to intergranular cracking, where single LMO particles detach from the surfaces of secondary particles without changing the overall morphology.[16] Conversely, the layered structure of NMC is prone to intragranular cracking, where stress radiates from the center to the surface of secondary particles along the boundaries of multiple primary particles, leading to the fragmentation of NMC particles into irregular spherical structures.[17] Compared to the pristine material, the higher specific surface area of degraded cathode mixture due to the fragmentation lower the resistance of Li^+ migration and enhance the rate capability. Although the morphologies of degraded and regenerated cathode mixture appeared consistent, a subtle increase in particle size after regeneration was observed, due to the agglomeration of smaller particles at high temperatures.

XRD was conducted to study the crystal structure recovery of the degraded cathode mixture in the regeneration process. Figure 3c illustrates XRD patterns of pristine LMO, pristine NMC111, and both the degraded and regenerated LMO/NMC cathode mixtures. The spinel structure of LMO is characterized by a standard pattern of the $Fd\bar{3}m$ space group, while the layered structure of NMC exhibits a standard pattern of the $R\bar{3}m$ space group, aligning well with the typical α-$NaFeO_2$ structure. The lithium loss in the degraded cathode mixture leads to a decrease in the lattice parameter of LMO, resulting in the (111) peak of LMO shifting to a higher angle. Conversely, the lithium deficiency in NMC causes an expansion of its crystal lattice along the *c*-axis, as reflected in the (003) peak shifting to a lower angle. Thus, the combined peak of the cathode mixture splits into two distinct peaks due to the different structural changes of degraded LMO and NMC. After the regeneration process, the split (111) and (003) peaks merge and revert to the original position, indicating the full restoration of lithium loss in the degraded cathode mixture. Compared to the regenerated cathode mixture, a higher I_{003}/I_{104} ratio is noted, mainly attributed to the structure degradation of NMC in degraded cathode mixture.[18] Additionally, a notable expansion in the spacing between the peaks of the (108)/(110) doublets is observed, primarily due to the contraction in lattice parameters along the *a*-axis of NMC. This contraction is attributed to the smaller effective ionic radii of Ni^{3+} compared to Ni^{2+}, compensating for the lithium deficiency within the crystal lattice of NMC. After regeneration, a reduction in the spacing between the (108)/(110) doublet peaks is observed, indicating the restoration of the stoichiometry of the degraded mixture and the reduction of Ni^{3+} to Ni^{2+} due to lithium re-intercalation into the crystal structure. Therefore, the lithium loss in the degraded cathode mixture was fully restored, and the structural degradation, primarily associated with NMC, was effectively reversed by the regeneration process, as evidenced by the XRD results.

To evaluate the cycling performance, the degraded, regenerated, and pristine LMO/NMC cathode mixtures were cycled within a voltage range of 2.7–4.2 V at a current density of 0.5 C after three formation cycles at 0.1 C. **Figure 4**a displays the first cycle charge/discharge curves for these mixtures. With a capacity degradation of over 60%, the degraded mixture only showed a substantially lower initial capacity of 39.6 mAh g^{-1}. Notably, due to lithium re-intercalation and structural recovery in the regeneration process, the regenerated cathode mixture

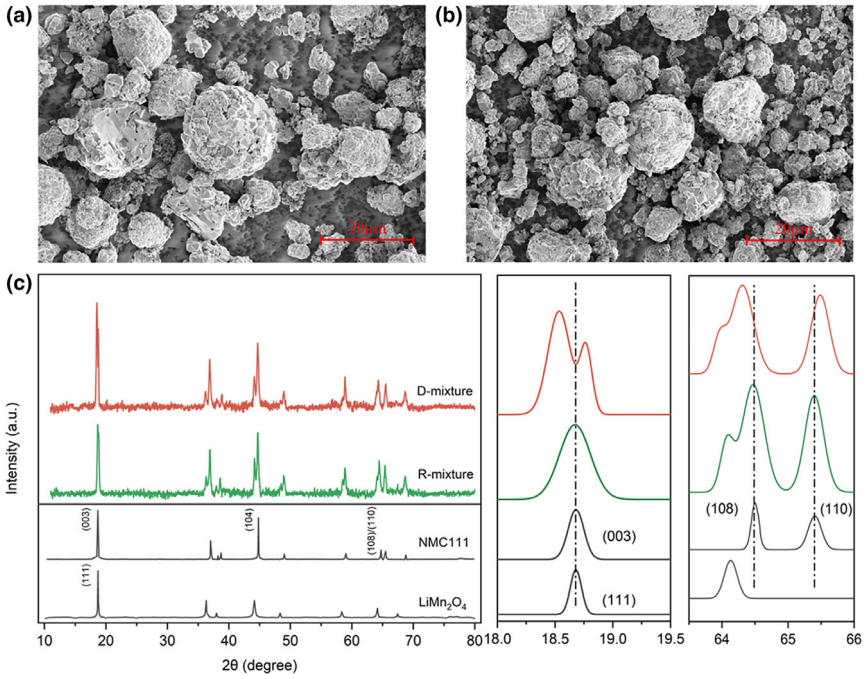

Figure 3. a) SEM image of the degraded mixture, b) SEM image of the regenerated mixture, c) XRD patterns of the pristine LMO, pristine NMC111, degraded and regenerated cathode mixtures.

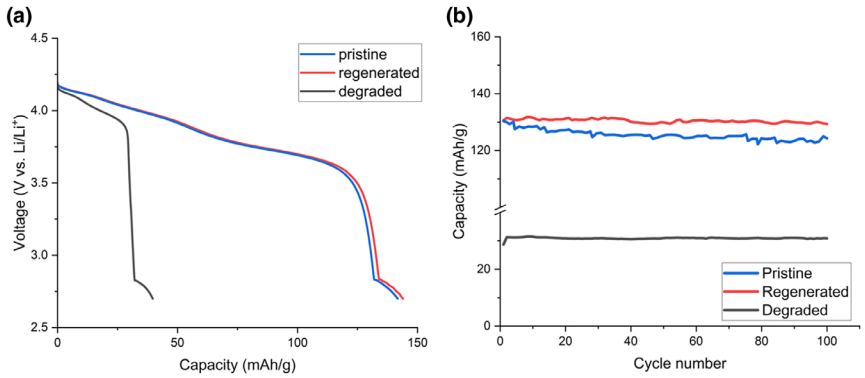

Figure 4. a) 1st cycle charging/discharging curves of the degraded and regenerated LMO/NMC cathode mixture, b) cycling performance of the degraded, regenerated, and pristine LMO/NMC cathode mixture.

showed an initial capacity of 144.0 mAh g^{-1}, marginally surpassing the 141.7 mAh g^{-1} of the pristine mixture. The enhanced capacity of the regenerated LMO/NMC cathode mixture can be attributed to the intercalation of a slightly excessive amount of lithium into the structure at a high temperature.[19–22] Furthermore, the low impedance of the regenerated mixture also contributes to the improvement in initial capacity.

Figure 4b presents the cycling performance of the degraded, regenerated, and pristine LMO/NMC cathode mixtures. Initially, at a current density of 0.5 C, the degraded, pristine, and regenerated mixtures delivered capacities of 31.2, 131.2, and 131.6 mAh g^{-1}, respectively. After 100 cycles, the pristine mixture maintained a capacity of 127.3 mAh g^{-1}, corresponding to a capacity retention of 97.0%. In comparison, the regenerated mixture demonstrated a slightly superior capacity of 128.3 mAh g^{-1}, with a capacity retention of 97.5%. The long-term cycling performance of the regenerated mixture at 1 C, shown in Figure S2, Supporting Information, reveals a remarkably stable cycling performance, maintaining a capacity of 127.3 mAh g^{-1} and a capacity retention of 95.1% after 250 cycles. The superior cycling performance of the regenerated cathode mixture, exceeding that of the pristine LMO/NMC mixture, is due to a low degree of cation mixing (relative to the approximately 6% in the pristine mixture) and diminished lithium residuals, achieved through washing steps in the regenerated LMO/NMC cathode mixture after the regeneration process.[23] Moreover, the electrochemical performance of the regenerated cathode mixture was enhanced by the restoration of the passive layer on the particle surface and a decrease in the Li^+ migration barrier.[24]

Figure 5a presents the rate capability of the degraded, pristine, and regenerated LMO/NMC cathode mixtures. The degraded LMO/NMC cathode mixture showed lower capacities, achieving only 40, 35, 25, 18, 10, and 2 mAh g^{-1} at current densities of 0.1, 0.2, 0.5, 1, 2, and 5 C, respectively. In contrast, the regenerated LMO/NMC cathode mixture exhibited substantially improved capacities at these current densities, delivering 140, 135, 132, 105, 83, and 50 mAh g^{-1}. When the current density was reverted to 0.1 C, the capacity of the regenerated mixture was fully restored to 140 mAh g^{-1}. Additionally, the regenerated LMO/NMC cathode mixture consistently demonstrated higher capacities at various current densities compared to the pristine mixture. This improvement is primarily attributed to the smaller particle size and larger specific surface area of the regenerated cathode mixture, as cathode particles fractured into smaller particles during the operational life of lithium-ion batteries. Given that the total weight and weight ratio of the cathode materials remain constant, the regenerated mixture, with reduced particle size, presents a larger surface area exposed to the electrolyte. This increased surface area facilitates simultaneous insertion of more lithium ions into the crystal structure, thereby improving the rate capability.[25–27] Moreover, the lower charge-transfer resistance observed in the regenerated cathode mixture, indicative of more efficient electrochemical kinetics, further supports the enhanced electrochemical performance at high rates.

Figure 5b illustrates the impedance distribution of the degraded, pristine, and regenerated LMO/NMC cathode mixtures. The contact resistances, as indicated by the intersection of the curves with the x-axis, were found to be similar for the degraded, regenerated, and pristine LMO/NMC cathode mixtures. The regenerated mixture

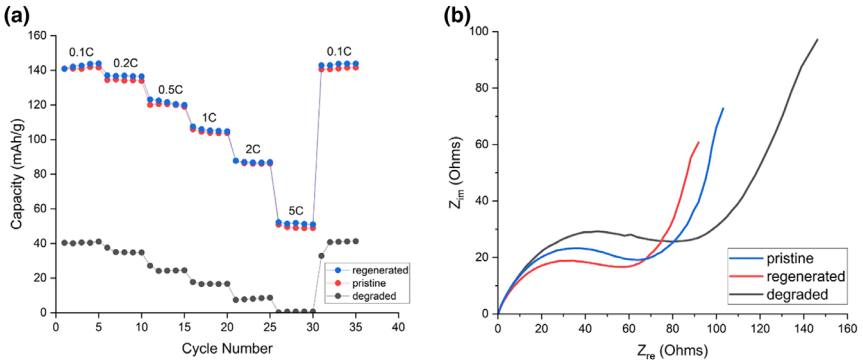

Figure 5. a) Rate capability of the degraded and regenerated LMO/NMC cathode mixtures, b) EIS of the degraded and regenerated LMO/NMC cathode mixtures.

demonstrated a slightly lower charge-transfer resistance compared to the pristine mixture. However, the charge-transfer resistance of the regenerated LMO/NMC cathode mixture was much lower than that of the degraded mixture. This reduction can be attributed to the decrease of cation mixing and elimination of lithium residuals on the surface of the cathode particles through the regeneration process. The recovered structure effectively reduced Li^+ migration barriers, resulting in a low charge-transfer resistance.

3. Life-Cycle Assessment and Industrial Application Prospective

In this paper, a cradle-to-grave life-cycle assessment (LCA) model has been developed to evaluate the environmental impacts of the closed-loop manufacturing of the lithium-ion battery packs using the regenerated LMO/NMC cathode mixture from spent EV batteries. A baseline battery pack using the pristine LMO/NMC cathode mixture is modeled for benchmarking.[28] Both of the battery packs are designed to have the same structure, capacity (64.5 kWh), and mass (417 kg). The analysis model is established in industrial-scale production, upscaled from lab data.

Energy consumption is first investigated in the developed direct recycling method for each step. As illustrated in **Figure 6**, 1.38 MJ energy is needed to regenerate 1 kg of the LMO/NMC cathode mixture material with a comparable electrochemical performance. Among all the steps, stirring consumes the most energy (0.73 MJ kg^{-1} regenerated LMO/NMC cathode mixture) since the NMP solution is continuously stirred and maintained at 60°C for 10 h. Meanwhile, vacuum drying is the second largest energy-intensive step and consumes 0.12 MJ kg^{-1} regenerated LMO/NMC cathode mixture. The preheating and sintering steps only require 9% and 8% of total energy consumption since the LMO/NMC was only treated at 300°C, which is low compared to typical direct recycling methods.[8] Compared to the pristine LMO/NMC cathode production which consumes 14.4 MJ kg^{-1} energy, the regeneration method shows a great potential in energy saving of 90.4%.[29] Additionally, the total cost of regenerated LMO/NMC cathode mixture is reduced by approximately 44% compared to the pristine cathode mixture per kilogram according to the EverBatt battery LCA model analysis.[30]

According to literature and experimental data, the LCA is performed with the functional unit set at 1 kg of the LMO/NMC-graphite battery pack and includes six stages: material extraction, material processing, battery manufacturing, cell & pack assembly, battery use, and end-of-life (EoL).[31] Employing Ecoinvent database and Sphera LCA, a comparative analysis is conducted between the regenerated and the baseline LMO/NMC-graphite battery packs using ReCiPe 2016 method to assess 13 different categories of environmental impacts, including GWP (Global warming), FDP (Fossil depletion), FETP (Freshwater ecotoxicity), POFP (Photochemical oxidant formation), HTP (Human toxicity), FEP (Freshwater eutrophication), MEP (Marine eutrophication), ODP (Ozone depletion), METP (Marine ecotoxicity), MDP (Metal Depletion), PMFP (Particulate matter formation), TAP (Terrestrial acidification), and TETP (Terrestrial ecotoxicity), as shown in **Figure 7**. The largest reduction occurs in TAP. The TAP of the baseline battery pack is 0.42 kg SO_2 eq. kg^{-1} battery pack while the TAP of the regenerated battery pack is 0.19 kg SO_2 eq. kg^{-1} battery pack, resulting in a 55% reduction of TAP. This is mainly because the regeneration of the LMO/NMC eliminates the material processing steps in producing pristine LMO and NMC which causes severe terrestrial acidification. The particulate matter formation is also greatly mitigated. The PMFP of the baseline battery pack is 0.13 kg PM2.5 eq. kg^{-1} battery pack while the PMFP of the regenerated battery pack is 0.065 kg PM2.5 eq. kg^{-1} battery pack. The LMO/NMC regeneration causes a 51% reduction in PM2.5 emission since the dusty steps in conventional LMO/NMC production are no longer needed, such as nickel sulfate production.

The comparative study reveals that the battery packs using the regenerated LMO/NMC cathode mixture have up to 55% lower environmental impacts than the baseline battery pack, except for MEP and ODP. The higher MEP and ODP values result from the newly introduced materials in the regeneration steps, such as lithium nitrate. Future advancements in direct recycling technologies for lithium-ion battery packs, which are presently under development at a lab scale, hold the

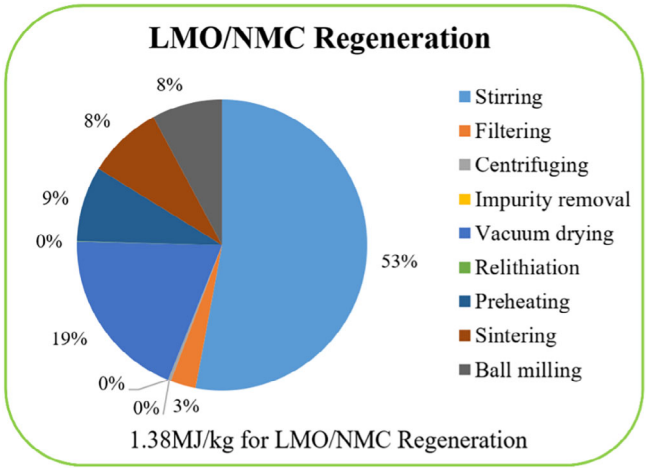

Figure 6. Energy consumption in the direct recycling method for the LMO/NMC cathode mixture.

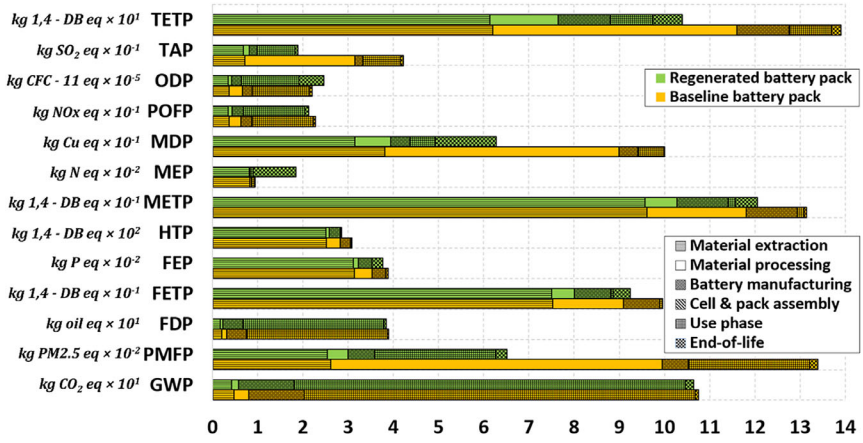

Figure 7. Benchmarking of Cradle-to-grave Life-Cycle Impacts between Baseline and Regenerated Battery Pack.

promise of significant reduction of environmental impacts. As these technologies evolve and mature, both material and energy efficiencies are expected to improve in the future.

The recycling industry for cathode materials requires a high-efficiency, low energy-consumption, and cost-effective process to maximize profit. However, there are still gaps in the scaling the proposed lab-scale recycling processes to meet industrial demands. The main challenges in scaling up direct recycling processes include 1) the inefficient extraction of degraded cathode particles from retired lithium-ion batteries, 2) the prolonged processing time and high usage of NMP (N-methyl-2-pyrrolidone) for removing residuals, and 3) the cost and availability of LiNO in the recycling processes.

In the proposed direct recycling processes, the extraction of degraded cathode particles involves discharging the retired battery packs, separating packs into individual cells, manually disassembling pouch cells, sorting cathode and anode electrodes, and removing binder materials. The lab-scale method for extraction takes approximately 30 h and requires an inert gas environment for safe operation, resulting in low efficiency. To address this for industrial applications, a mechanical crushing process, which opens the battery cell housing and transforms battery packs into bulk materials, can replace the current low-efficiency method.[32] The mechanical crushing process does not require a specific gas environment, and battery crushing can be completed within minutes.[33] Degraded cathode particles can then be simply retrieved using magnetic sorting techniques.[34] By incorporating mechanical crushing, the extraction efficiency for cathode particles can be significantly improved for industrial-scale recycling.

After extraction, residual materials, including PVDF (polyvinylidene fluoride) and carbon black, remain on the degraded cathode particles. In lab-scale processes, PVDF is removed by dissolving it in a significant amount of NMP, which is much more than used in electrode manufacturing.[35] Overnight stirring is also required to fully dissolve the PVDF. This approach is time-consuming and cost-ineffective. Furthermore, a subsequent centrifuge process is needed to separate the cathode particles from carbon black. Since PVDF decomposes at 350°C[36] and carbon black burns at 400°C,[37] a short heating process at 400°C for 20 min can effectively remove both materials. This heating process eliminates the need for toxic NMP, reducing both costs and processing time, thus making the method more viable for industrial applications.

LiNO is an easily synthesized chemical widely used in industry and is selected as the lithium source due to its low melting point, enabling low-temperature sintering. Although LiNO is more expensive than other lithium salts, it ensures low energy consumption in the direct recycling processes. To further reduce costs, lower cost salts such as LiOH, KOH, and Li CO could be used to form a eutectic salt system that lowers the melting point.[38,39] However, a recycling system might be required to recover non-lithium salts, ensuring the process remains efficient and cost-effective.

Other steps in the direct recycling process, such as sintering, washing, and filtering, are already widely used in industrial applications and can be easily adapted for larger-scale processes. With these alternative processes in place, the current lab-scale direct recycling methods can be successfully scaled up to industrial levels, offering a high degree of energy and cost-efficiency.

4. Conclusion

In this study, a direct recycling method was developed to recycle the degraded LMO/NMC cathode mixtures from retired EV battery packs that had undergone over 60% capacity degradation in the past EV operations. This regeneration process was carried out at a low sintering temperature, eliminating the need for any specific gas environment. Through this approach, the degraded LMO/NMC cathode mixture with significant capacity fading and lithium loss was effectively regenerated to the same level as pristine material in terms of the chemical composition and crystal structure. Remarkably, the regenerated LMO/NMC cathode mixture shows a specific capacity of 144.0 mAh g^{-1} and maintains 95.1% capacity after 250 cycles. Additionally, the regenerated cathode mixture delivers a capacity of 83 mAh g^{-1} at 2 C, which is slightly higher than that of pristine materials due to the low charge-transfer resistance. The reduction of charge-transfer resistance in the regenerated cathode mixture is attributed to the elimination of the passive layer on the particle surface during the direct recycling process. Life-cycle assessment results reveal a 90% reduction in energy consumption and 51% less PM2.5 emissions for lithium-ion battery packs manufactured with the direct recycled cathode mixture compared to pristine materials produced by conventional fabrication processes. Additionally, the potential challenges and strategies for scaling the proposed direct recycling processes to an industrial level are also discussed. This method demonstrates clear advantages for sustainable and cost-effective battery recycling. The successful regeneration of the degraded cathode mixture through this direct recycling method underscores its practical viability for industrial applications, highlighting the potential of low-temperature direct recycling in the battery recycling industry.

5. Experimental Section

Pouch-cell disassembly: The spent pouch cells utilized in this study were extracted from a retired battery pack of a Chevrolet Volt. Before disassembly, the pouch cells were fully discharged to 2.6 V for safety. The teardown of the pouch

cells was conducted in an argon-filled glovebox. During this process, the cathode and anode electrodes were carefully sorted and collected for further recycling procedures.

Materials extraction and regeneration: The cathode electrodes were immersed in Dimethyl Carbonate (DMC, Sigma Aldrich) for 30 min to dissolve the residual electrolyte. Subsequently, the electrodes were cleaned with acetone to remove the residual separators. Then, the electrodes were stirred in the N-Methylpyrrolidone (NMP, Sigma Aldrich) to dissolve the Polyvinylidene Fluoride (PVDF) and facilitate the detachment of cathode materials from the current collectors. The active materials and conductive agents were segregated based on density differences in the high-speed centrifuge (ST 8, Thermo Fisher), with the degraded LMO/NMC cathode mixture settling at the bottom of the solution and carbon black floating on top. To eliminate the impurities, such as the aluminum debris, the degraded mixture was soaked and stirred in the NaOH solution for a few minutes. The degraded mixture was rinsed with distilled water several times and dried in the vacuum oven.

The degraded cathode mixture was mixed with excessive $LiNO_3$ in the ball milling machine (SFM-3, MTI) for 10 min. Then, the mixture was preheated at 150°C for 2 h and sintered in the muffle furnace (KSL-1700X-KA, MTI) at 300°C for 4 h under the air flow. The ramping rate of the heating process is 5°C min^{-1}. After sintering, the cathode mixture was washed with distilled water three times to dissolve the residual lithium salts. The LMO/NMC cathode mixture was obtained by drying the powder in the vacuum oven (DZF-602,0 MTI) at 120°C for 2 h.

Coin-cell assembly: CR2032-type coin cells were fabricated using the regenerated LMO/NMC mixture as the cathode material and lithium foil as the counter electrode. For the electrode preparation, both degraded and regenerated LMO/NMC cathode were mixed with carbon black (Super P65, MTI), and polyvinylidene difluoride (PVDF, MTI) in a mass ratio of 8:1:1 in NMP to form uniform slurries. The slurries were cast on the aluminum foil using a doctor blade and vacuum coating machine (MSK-AFA-II-VC, MTI). The coated electrodes were dried in the vacuum oven at 110°C for 10 h. Subsequently, the electrodes were cut into discs and calendered using a rolling machine (MSK-2150, MTI). The cathode electrodes achieved an active mass loading of approximately 3 mg cm^{-2}. 1.2 M $LiPF_6$ in EC: EMC: DMC (1:1:1 wt%) was used as the electrolyte, and monolayer membrane (Celgard 2500, MTI) was used as the separator. The assembly of CR2032-type coin cells was conducted in an argon-filled glovebox (LABmaster Pro, MBRAUN).

Material characterization: The crystal structures of the degraded cathode mixture and the regenerated cathode mixture were measured by X-ray diffraction (XRD) using the HyPix-3000 Detector with a scanning rate of 0.58 deg/min. The morphology of the degraded and regenerated mixture was observed by scanning electron microscope (SEM, FEI Quanta 3D).

Electrochemical characterization: The electrochemical performance of CR2032-type coin cells was evaluated on the Neware Battery Tester (Neware LLC). The cycling performance and rate capability tests were conducted at a voltage range of 2.7–4.2 V. For the cycling performance test, the cells underwent three formation cycles at 0.1 C, followed by 100 cycles at 0.5 C. Rate capability was evaluated at current densities of 0.1, 0.2, 0.5, 1, 2, and 5 C. The electrochemical impedance spectroscopy (EIS) measurements for both degraded and regenerated LMO/NMC cathodes were performed using a potentiostat (VersaSTAT 3F, AMETEK SI).

Acknowledgements

Financial support from the US National Science Foundation (CBET-2101129) is acknowledged.

Conflict of Interest

The authors declare no conflict of interest.

Supporting Information

Supporting Information is available from the Wiley Online Library or from the author.

Keywords

direct recycling, life-cycle assessment, lithium-ion battery, spent cathode mixture

Received: July 30, 2024
Revised: September 9, 2024
Published online: November 26, 2024

[1] W. Li, X. Liu, H. Celio, P. Smith, A. Dolocan, M. Chi, A. Manthiram, *Adv. Energy Mater.* **2018**, *8*, 1703154.
[2] Z. Tong, M. Wang, Z. Bai, H. Li, N. Wang, *ChemPhysMater* **2024**, DOI: 10.1016/j.chphma.2024.05.005.
[3] B. Makuza, Q. Tian, X. Guo, K. Chattopadhyay, D. Yu, *J. Power Sources* **2021**, *491*, 229622.
[4] A. Chagnes, B. Pospiech, *J. Chem. Technol. Biotechnol.* **2013**, *88*, 1191.
[5] C. Wu, M. Xu, C. Zhang, L. Ye, K. Zhang, H. Cong, L. Zhuang, X. Ai, H. Yang, J. Qian, *Energy Storage Mater.* **2023**, *55*, 154.
[6] H. Gao, Q. Yan, P. Xu, H. Liu, M. Li, P. Liu, J. Luo, Z. Chen, *ACS Appl. Mater. Interfaces* **2020**, *12*, 51546.
[7] X. Meng, J. Hao, H. Cao, X. Lin, P. Ning, X. Zheng, J. Chang, X. Zhang, B. Wang, Z. Sun, *Waste Manag.* **2019**, *84*, 54.
[8] X. Yu, S. Yu, Z. Yang, H. Gao, P. Xu, G. Cai, S. Rose, C. Brooks, P. Liu, Z. Chen, *Energy Storage Mater.* **2022**, *51*, 54.
[9] L. Wuschke, H. G. Jäckel, T. Leißner, U. A. Peuker, *Waste Manag.* **2019**, *85*, 317.
[10] L. Brückner, J. Frank, T. Elwert, *Metals* **2020**, *10*, 1107.
[11] S. B. Chikkannanavar, J. H. Kim, W. Jung, in *Transition Metal Oxides for Electrochemical Energy Storage* (Eds: V. Augustyn, J. Nanda), Wiley, Hoboken, NJ **2022**, pp. 257–72.
[12] L. Britala, M. Marinaro, G. Kucinskis, *J. Energy Storage* **2023**, *73*, 108875.
[13] A. H. Marincaş, F. Goga, S. A. Dorneanu, P. Ilea, *J. Solid State Electrochem.* **2020**, *24*, 473.
[14] P. N. Suryadi, J. Karunawan, O. Floweri, F. Iskandar, *J. Energy Storage* **2023**, *68*, 107634.
[15] Y. Chen, S. Song, X. Zhang, Y. Liu, *J. Phys. Conf. Ser.* **2019**, *1347*, 012012.
[16] F. P. McGrogan, S. N. Raja, Y. M. Chiang, K. J. Van Vliet, *J. Electrochem. Soc.* **2018**, *165*, A2458.
[17] K. Mao, Y. Yao, Y. Chen, W. Li, X. Shen, J. Song, H. Chen, W. Luan, K. Wu, *J. Energy Storage* **2024**, *84*, 110807.
[18] S. K. Jung, H. Gwon, J. Hong, K. Y. Park, D. H. Seo, H. Kim, J. Hyun, W. Yang, K. Kang, *Adv. Energy Mater.* **2014**, *4*, 1300787.
[19] T. Wang, H. Luo, Y. Bai, I. Belharouak, K. Jayanthi, M. P. Paranthaman, B. T. Manard, E. T.-H. Wang, F. Dogan, S.-B. Son, B. J. Ingram, Q. Dai, S. Dai, *J. Power Sources* **2024**, *593*, 233798.
[20] W. M. Dose, S. Kim, Q. Liu, S. E. Trask, A. R. Dunlop, Y. Ren, Z. Zhang, T. T. Fister, C. S. Johnson, *J. Mater. Chem. A* **2021**, *9*, 12818.
[21] V. A. Godbole, J. F. Colin, P. Novák, *J. Electrochem. Soc.* **2011**, *158*, A1005.
[22] S. Y. Luchkin, M. A. Kirsanova, D. A. Aksyonov, S. A. Lipovskikh, V. A. Nikitina, A. M. Abakumov, K. J. Stevenson, *ACS Appl. Energy Mater.* **2022**, *5*, 7758.
[23] W. Zhao, L. Zou, H. Jia, J. Zheng, D. Wang, J. Song, C. Hong, R. Liu, W. Xu, Y. Yang, J. Xiao, C. Wang, J. G. Zhang, *ACS Appl. Energy Mater.* **2020**, *3*, 3369.
[24] Y. Qian, P. Niehoff, M. Börner, M. Grützke, X. Mönnighoff, P. Behrends, S. Nowak, M. Winter, F. M. Schappacher, *J. Power Sources* **2016**, *329*, 31.
[25] A. Soloy, D. Flahaut, J. Allouche, D. Foix, G. Salvato Vallverdu, E. Suard, E. Dumont, L. Gal, F. Weill, L. Croguennec, *ACS Appl. Energy Mater.* **2022**, *5*, 5617.
[26] A. C. Wagner, N. Bohn, H. Geßwein, M. Neumann, M. Osenberg, A. Hilger, I. Manke, V. Schmidt, J. R. Binder, *ACS Appl. Energy Mater.* **2020**, *3*, 12565.
[27] A. S. Wijareni, H. Widiyandari, A. Purwanto, A. F. Arif, M. Z. Mubarok, *Energies* **2022**, *15*, 5794.
[28] J. B. Dunn, L. Gaines, J. Sullivan, M. Q. Wang, *Environ. Sci. Technol.* **2012**, *46*, 12704.

[29] S. Ahmed, P. A. Nelson, K. G. Gallagher, N. Susarla, D. W. Dees, *J. Power Sources* **2017**, *342*, 733.
[30] X. Wu, Y. Liu, J. Wang, Y. Tan, Z. Liang, G. Zhou, *Adv. Mater.* **2024**, *36*, 2403818.
[31] K. Shen, C. Yuan, M. Hauschild, *CIRP Ann.* **2023**, *72*, 13.
[32] J. Diekmann, S. Sander, G. Sellin, M. Petermann, A. Kwade, in *Recycling of Lithium-Ion Batteries: The LithoRec Way* (Eds: A. Kwade, J. Diekmann), Springer, Cham, Switzerland **2018**, pp. 127–38.
[33] A. Vanderbruggen, J. Sygusch, M. Rudolph, R. Serna-Guerrero, *Colloids Surf. A Physicochem. Eng. Asp.* **2021**, *626*, 127111.
[34] D. N. Shibaeva, A. A. E. Kompanchenko, S. V. E. Tereschenko, *Fortschr. Mineral.* **2021**, *11*, 797.
[35] M. Ahuis, A. Aluzoun, M. Keppeler, S. Melzig, A. Kwade, *J. Power Sources* **2024**, *593*, 233995.
[36] M. Bhar, S. Ghosh, S. Krishnamurthy, Y. Kaliprasad, S. K. Martha, *RSC Sustain.* **2023**, *1*, 1150.
[37] Z. Meng, D. Yang, Y. Yan, *J. Therm. Anal. Calorim.* **2014**, *118*, 551.
[38] J. Yang, W. Wang, H. Yang, D. Wang, *Green Chem.* **2020**, *22*, 6489.
[39] H. Yang, B. Deng, X. Jing, W. Li, D. Wang, *Waste Manag.* **2021**, *129*, 85.